Supplementary Data

Bacterial initiators form dynamic filaments on single-stranded DNA monomer by monomer

Hsin-Mei Cheng, Philip Gröger, Andreas Hartmann, and Michael Schlierf*

Affiliation: B CUBE – Center for Molecular Bioengineering, TU Dresden, Arnoldstr. 18, 01307 Dresden, Germany

Correspondence: schlierf@bcube-dresden.de

Different nucleotides affect the DnaA ssDNA interaction

The FRET changes of the pdT21 based on DnaA binding was monitored in ensemble experiments with a LS55 Fluorescence Spectrometer (Perkin Elmer). 25 nM of pdT21 or HR13 DNA substrate and 10 μM of DnaA in the binding buffer (20 mM Tris-HCl pH 8.0, 100 mM NaCl, 10 mM $MgCl_2$, 0.1 mg/ml BSA) and 2 mM ADP•BeF_3, ATP, ATPγS, and ADP, respectively were used. The sample was excited with 530 nm (5 nm excitation slit) and the emission was scanned from 545 to 750 nm (5 nm emission slit).

The ensemble FRET experiment agreed well with previous FRET experiments. DnaA binds ssDNA successfully with a drop in FRET efficiency in the presence of ADP•BeF_3 (Supplementary Figure S1A), ATPγS, and ATP (Supplementary Table S1) (1). The FRET efficiency enhancement in the presence of ADP and without nucleotide condition is probably due to protein dye interaction (2).

In the single-molecule FRET experiments, we added DnaA in the presence of ATP and the analogues (ADP•BeF_3, ATPγS, AMPPCP, and AMPPNP). Single molecule time traces showed in all cases FRET efficiency fluctuations with similar kinetics (Supplementary Figure S1B-E). Compared to RecA, which forms a stable filament on ssDNA in the presence of ATPγS, a slowly-hydrolyzed ATP analogue (3), DnaA binds and unbinds dynamically. Experiments with ATP in solution exhibited a reduced fraction of active molecules over time of a few minutes, possibly due to ATP hydrolysis and inactivation of DnaA molecules in the DnaA-ADP state (Supplementary Figure S1H) (4). Therefore, we decided to perform our experiments with the ATP analogue ADP•BeF_3. In the presence of ADP or absence of any nucleotide, fluctuations in the FRET traces were not observed (Supplementary Figure S1F-G).

DnaA does not unwind dsDNA

To exclude that the observed FRET fluctuations are caused by partial melting of the duplex stem in the pdT21 substrate, we performed a set of control experiments with a modified substrate pdTcontrol. In pdTcontrol the donor and the acceptor fluorophores were labeled at the ss-dsDNA junction (Supplementary Figure S2A). If DnaA unwinds the dsDNA stem even by only a few nucleotides, we would expect a drop in the FRET efficiency. However, the addition of DnaA with 1 mM ADP•BeF_3 did not result in any significant changes in the FRET efficiency histograms and on the single-molecule level (Supplementary Figure S2B). We conclude DnaA is not able to actively melt the dsDNA stem of our DNA substrate within our experimental time frame. Furthermore, the FRET fluctuations observed in the reported FRET experiments with the donor and acceptor fluorophores separated by ssDNA are therefore due to stretching of ssDNA by protein ssDNA interactions.

FRET efficiency for HR substrates in DNA only condition

The FRET histograms of the bare HR13, HR10 and HR7 substrates show transfer efficiencies of 0.7, 0.75, and 0.8, respectively (Supplementary Figure S4A). The highest FRET values from the transition density plots (Figure 3) for these three HR substrates (0.67, 0.73, and 0.76 for HR13, HR10, and HR7, respectively) agree very well with the FRET efficiencies in the bare DNA condition and are thus identified as state 0 without any DnaA bound between donor and acceptor fluorophores.

Transition rates between two neighboring FRET states of the HR and HR-box substrates

Transition kinetics of DnaA-ADP•BeF_3 and DnaA-ATP on HR13 were found to be identical within error (Figure 3C and supplementary Figure S4G). DnaA-ATP activity decreased over a few minutes rapidly due to ATP hydrolysis (Supplementary Figure S1H). Supplementary

Table S2 shows the transition rates ($k_{on(obs)}$ and k_{off}) for the highly populated states of HR substrates are between 0.4-0.6 s^{-1}. The binding rates k_{on} were calculated as $k_{on(obs)}$ divided by DnaA concentration (5 μM in our experiment). The dissociation constant K_D is determined as k_{off}/k_{on}. After calculation, the K_D is approximately 5 μM.

Comparing the binding rates $k_{on(obs)}$ for HR13, HR13-2box, and HR13-5box, the binding rate of the first monomer (transition 0→1) increases after adding DnaA boxes, indicating the filament formation improved. With longer boxes, the first monomer between donor and acceptor is stabilized such that unbinding (1→0) and rebinding (0→1) was not observed.

PAGE based band shift assay

We performed fluorescence EMSA (electrophoretic mobility shift assay) in the smFRET experiment buffer to determine the dissociation constants for the DnaA-ssDNA interaction. Different amount of DnaA was incubated with 1 pmole HR13, OP13, dT21-ssDNA, or 18bp-stem substrates for 5 minutes at room temperature in the presence of 1mM ADP•BeF_3, 20 mM Tris-HCl, 100 mM NaCl, 10 mM $MgCl_2$, and 1 mg/mL BSA and glycerol. The quantified bands (Aida image analyzer) were fitted with equation 1 to determine the dissociation constant and the cooperativity.

$$\phi = \left[\frac{1}{1+(K_D/[P_t])^n}\right] \qquad (1)$$

ϕ represents the bound fraction, K_D is the dissociation constant, $[P_t]$ is the protein concentration, and n is the Hill coefficient. dT21-ssDNA and 18bp-stem are control substrates designed for examining if the dsDNA region of our partial duplex DNA substrates influences the DnaA binding to the ssDNA tail. In the presence of ADP•BeF_3, the extracted dissociation constant is ~ 1.6-2 μM for HR13, OP13, and dT21-ssDNA conditions. For the pure duplex DNA the dissociation constant was determined to be about 3 to 4 times higher K_D = 6.5 μM

for 18bp-stem (Supplementary Figure S6), suggesting that the duplex stem of the DNA substrates has a minor influence on DnaA-ssDNA interactions.

Supplementary References

1. Duderstadt, K.E., Chuang, K. and Berger, J.M. (2011) DNA stretching by bacterial initiators promotes replication origin opening. *Nature*, **478**, 209-U291.

2. Hwang, H. and Myong, S. (2014) Protein induced fluorescence enhancement (PIFE) for probing protein-nucleic acid interactions. *Chem. Soc. Rev.*, **43**, 1221-1229.

3. Joo, C., McKinney, S.A., Nakamura, M., Rasnik, I., Myong, S. and Ha, T. (2006) Real-time observation of RecA filament dynamics with single monomer resolution. *Cell*, **126**, 515-527.

4. Speck, C. and Messer, W. (2001) Mechanism of origin unwinding: sequential binding of DnaA to double- and single-stranded DNA. *EMBO J.*, **20**, 1469-1476.

5. Duderstadt, K.E., Mott, M.L., Crisona, N.J., Chuang, K., Yang, H. and Berger, J.M. (2010) Origin Remodeling and Opening in Bacteria Rely on Distinct Assembly States of the DnaA Initiator. *J. Biol. Chem.*, **285**, 28229-28239.

6. Ozaki, S. and Katayama, T. (2012) Highly organized DnaA-oriC complexes recruit the single-stranded DNA for replication initiation. *Nucleic Acids Res.*, **40**, 1648-1665.

7. Erzberger, J.P., Mott, M.L. and Berger, J.M. (2006) Structural basis for ATP-dependent DnaA assembly and replication-origin remodeling. *Nat. Struct. Mol. Biol.*, **13**, 676-683.

Figure S1

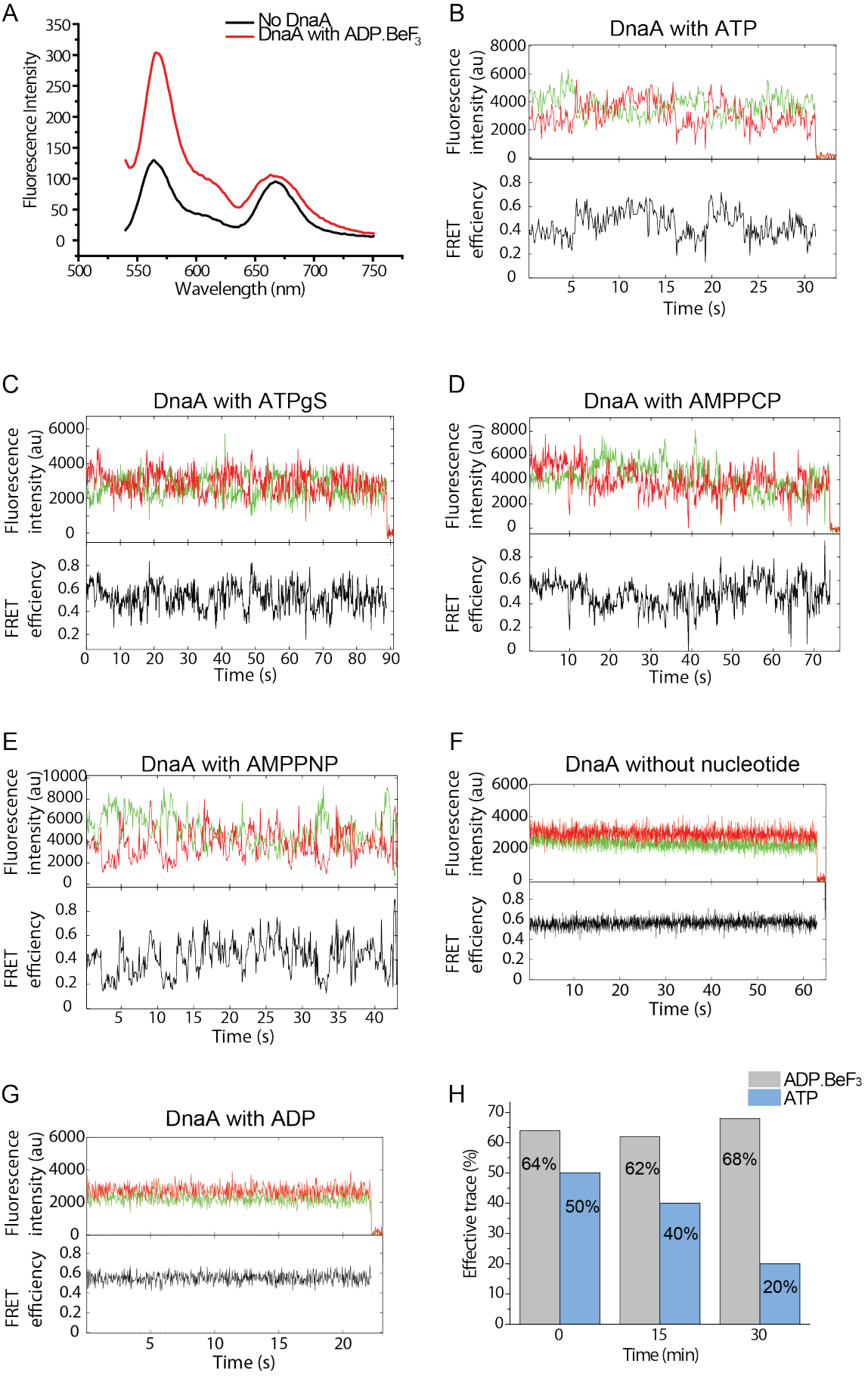
A
No DnaA
DnaA with ADP.BeF3
Fluorescence Intensity
Wavelength (nm)
B
DnaA with ATP
Fluorescence intensity (au)
FRET efficiency
Time (s)
C
DnaA with ATPgS
D
DnaA with AMPPCP
E
DnaA with AMPPNP
F
DnaA without nucleotide
G
DnaA with ADP
H
ADP.BeF3
ATP
Effective trace (%)
64%
50%
62%
40%
68%
20%
Time (min)

Supplementary Figure S1. Different nucleotides affect the DnaA ssDNA interaction.

(A) Ensemble fluorescence spectra of pdT21 in absence (black) and presence (red) of 10 μM DnaA and 2 mM ADP•BeF_3. Upon DnaA binding, the FRET efficiency changes significantly.(B)-(E) DnaA dynamically binds and unbinds to ssDNA in the presence of ATP (B), ATPγS (C), AMPPCP (D), and AMPPNP (E). Without nucleotides (F) or in the presence of ADP (G), FRET fluctuations were not observed. (H) The ratio of effective traces with FRET fluctuations for HR13 in the ADP•BeF_3 (grey) or ATP (blue) conditions over time. In the presence of ADP•BeF_3, the effective traces remain constant over 30 min. In the ATP condition, the effective traces decrease significantly within 30 min.

Figure S2

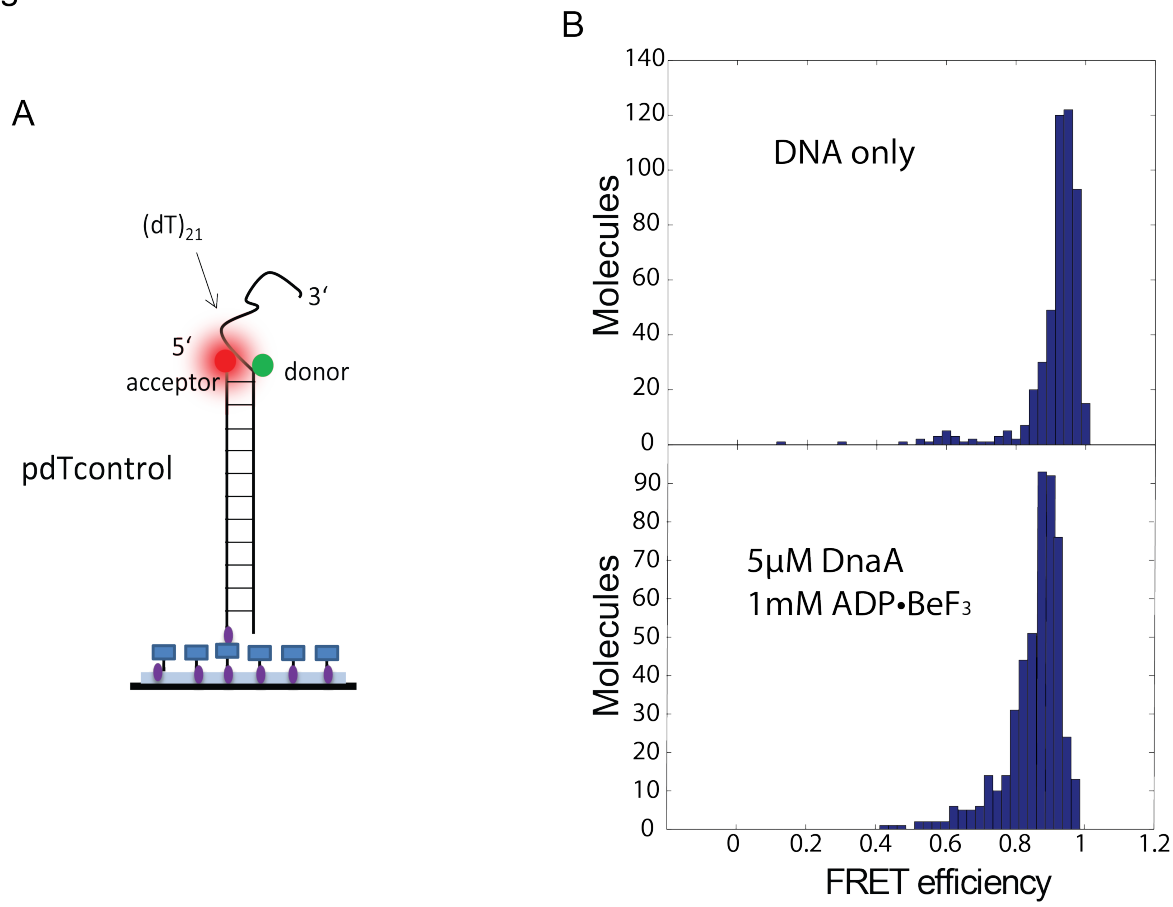

Supplementary Figure S2. Control experiment with pdTcontrol substrate

(A) pdTcontrol DNA substrate with the donor and acceptor labeled at the ss-dsDNA junction.

(B) The FRET histograms for pdTcontrol in the absence (top, 488 molecules) and presence (bottom, 495 molecules) of the 5 μM DnaA and 1 mM ADP•BeF_3.

Figure S3

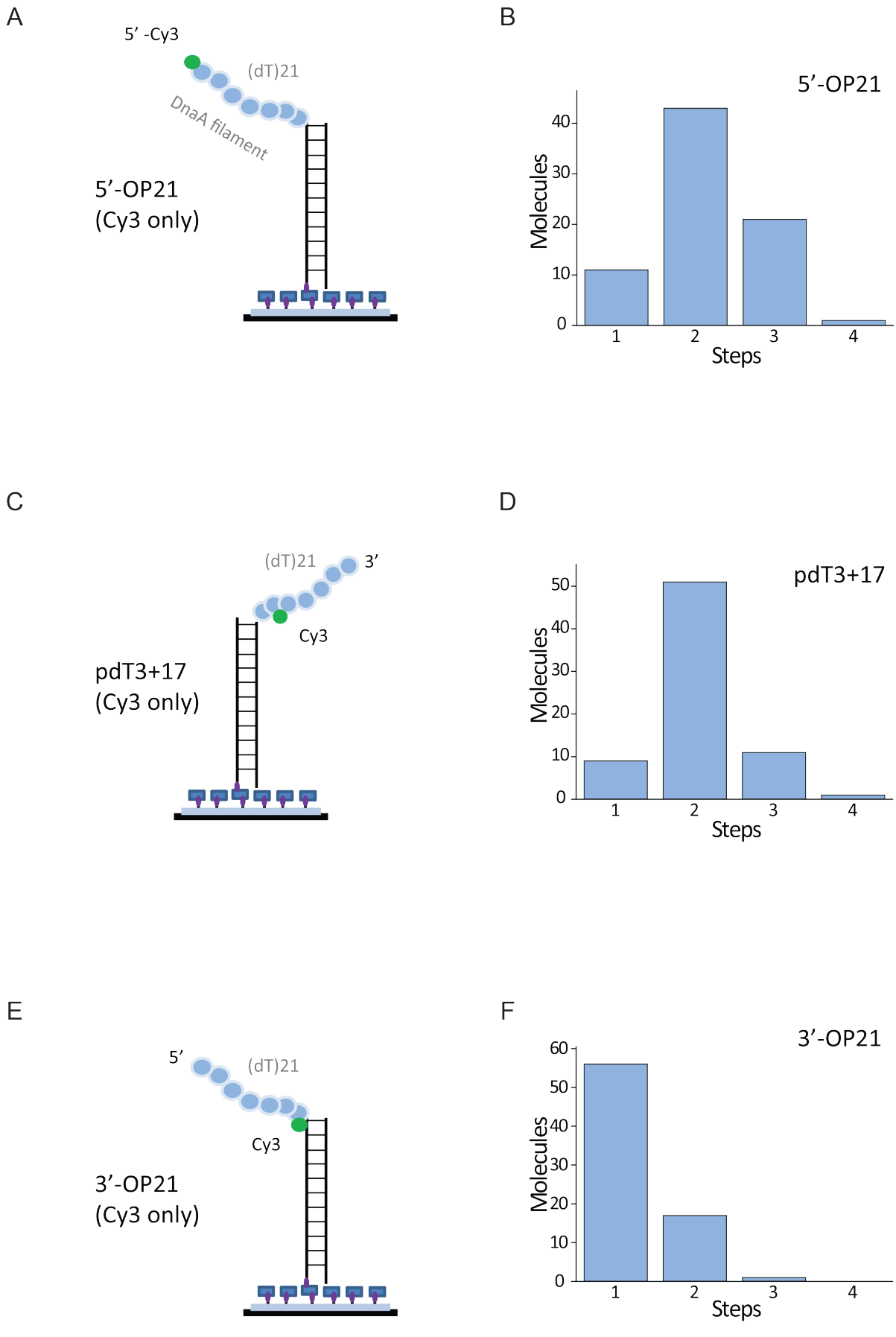
A
5' -Cy3
(dT)21
DnaA filament
5'-OP21
(Cy3 only)
B
5'-OP21
Molecules
Steps
C
(dT)21
3'
Cy3
pdT3+17
(Cy3 only)
D
pdT3+17
Molecules
Steps
E
5'
(dT)21
Cy3
3'-OP21
(Cy3 only)
F
3'-OP21
Molecules
Steps

Supplementary Figure S3. Control experiments for 5' end PIFE

(A) The partial duplex DNA substrate based on pdT21 (Cy3 only) but with opposite direction (5'-OP21).
(B) The histogram for 5'-OP21 shows that on average the number of steps from the initial intensity state to the highest intensity state is 2.2.
(C) The partial duplex DNA substrate based on pdTcontrol (Cy3 only) but the Cy3 labeling position is shifted by three nucleotides from the ss-ds junction (pdT3+17).
(D) The histogram for pdT3+17 shows that on average the number of steps from the initial intensity state to the highest intensity state is 2.1.
(E) The partial duplex DNA substrate based on pdTcontrol (Cy3 only) but with opposite direction (3'-OP21).
(F) The histogram for 3'-OP21 shows that the majority of traces exhibited a one state behavior.

Figure S4

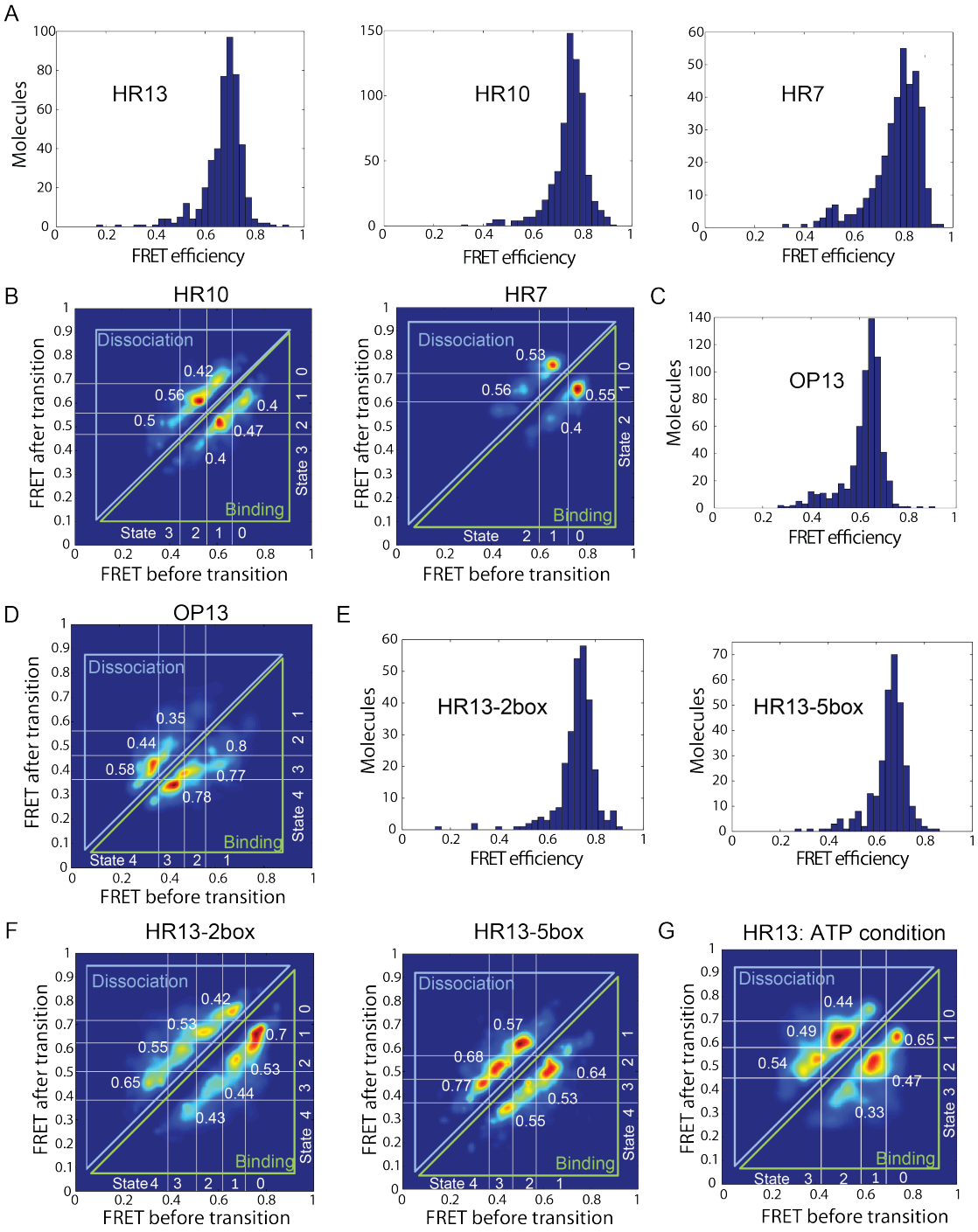
A
HR13
HR10
HR7
Molecules
FRET efficiency
B
HR10
HR7
Dissociation
Binding
FRET after transition
FRET before transition
C
OP13
D
OP13
E
HR13-2box
HR13-5box
F
HR13-2box
HR13-5box
G
HR13: ATP condition

Supplementary Figure S4. The smFRET results for different DNA substrates

(A) The FRET histograms for HR substrates in bare DNA condition. The FRET efficiency is ~ 0.7, 0.75, and 0.8 for HR13 (458 molecules), HR10 (676 molecules), and HR7 (365 molecules), respectively

(B) Left: A heat-map transition density plot (TDP) for HR10. (The same information as Fig. 3D) Right: The TDP for HR7. (The same information as Fig. 3E).

(C) The FRET histogram for OP13 substrate in DNA only condition shows the FRET efficiency is ~0.7 (606 molecules).

(D) The TDP for OP13. (The same information as Fig. 4C)

(E) The FRET histograms for HR-box substrates in DNA only condition show the FRET efficiency is ~0.75 and 0.68 for HR13-2box (271 molecules) and HR13-5box (308 molecules), respectively.

(F) Left: The TDP for HR13-2box. (The same information as Fig. 5B). Right: The TDP for HR13-5box (The same information as Fig. 5C)

(G) The TDP for HR13 in the presence of 1 mM ATP (80 FRET time traces, 502 transitions). Four different FRET states (peaks) with the FRET efficiency values of 0.72, 0.62, 0.51, and 0.39 are identified. The transition rates per second of each transition are represented next to each island.

Figure S5

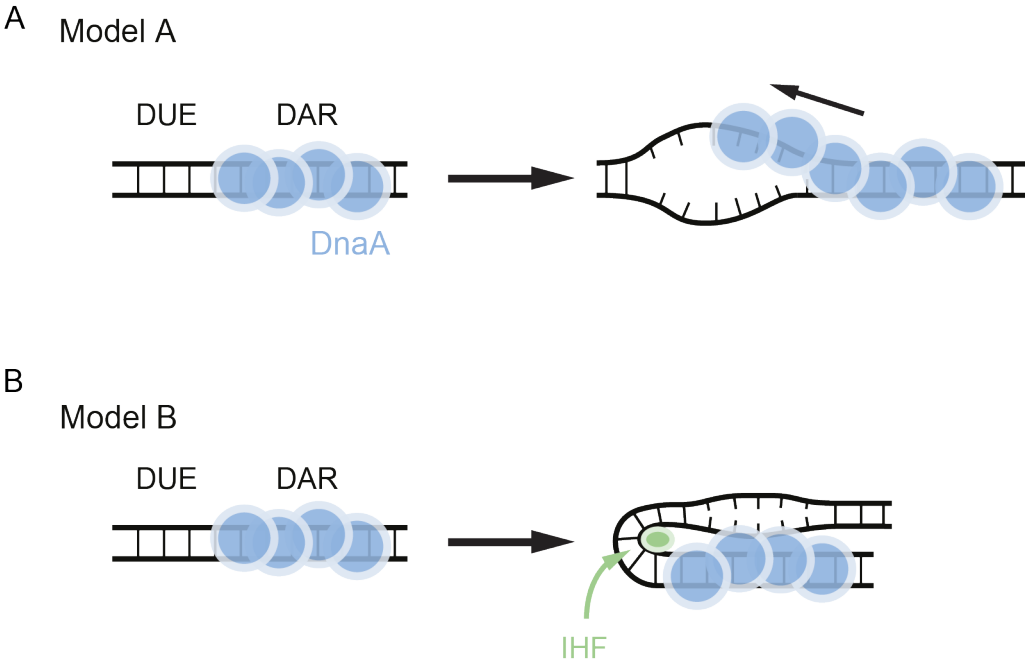

Supplementary Figure S5. Two different models for *oriC* melting by DnaA.

(A) In Model A, a continuous filament of DnaA ranging from the DnaA assembly region (DAR) to the DNA unwinding element (DUE) binding dsDNA and ssDNA, repectively (4,5).

(B) In Model B, the DnaA assembly occurs at DAR. In the presence of IHF, the DNA bends and allows the identical DnaA monomers to bind to single-stranded DUE (6).

Figure S6

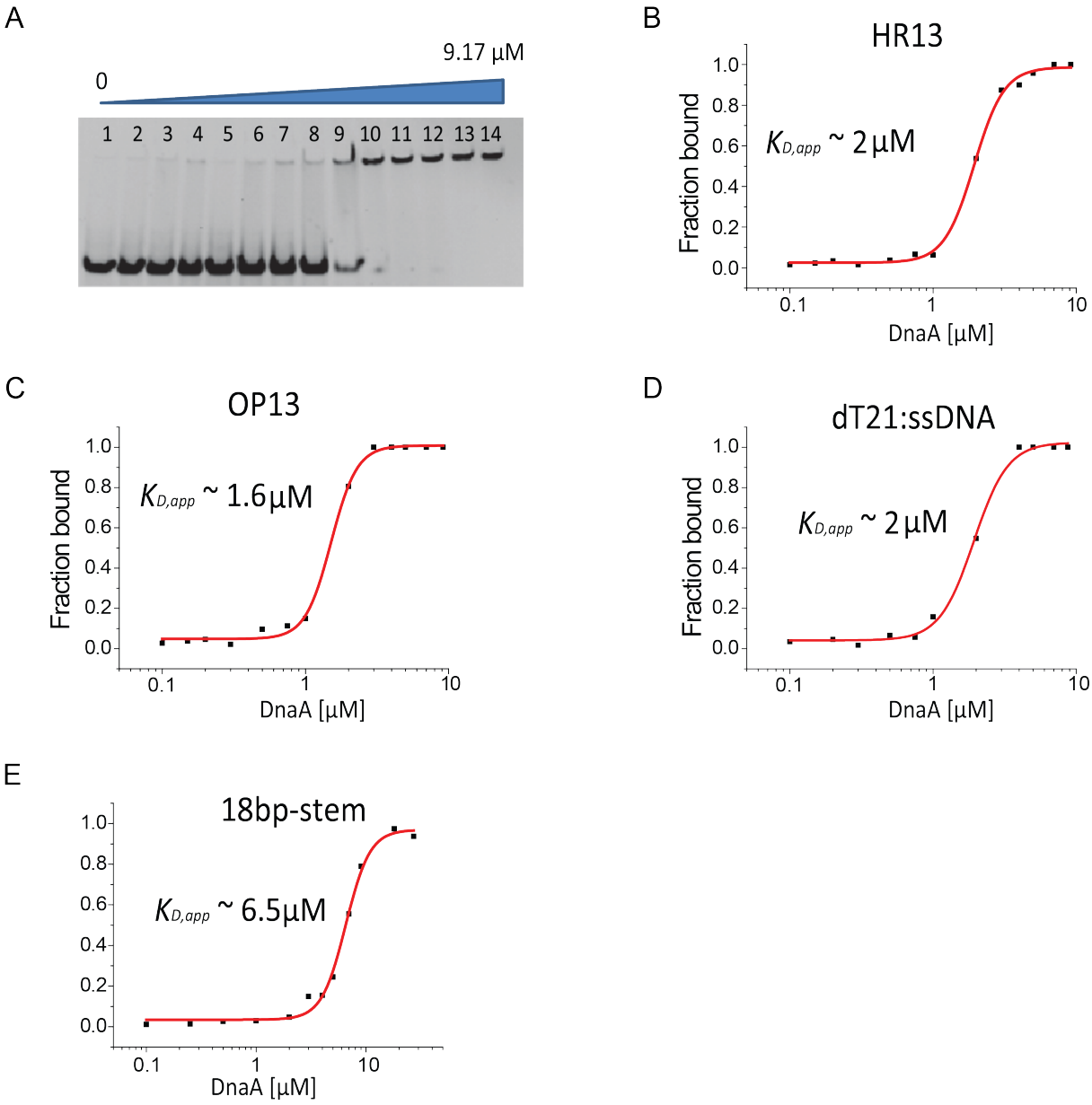

Supplementary Figure S6. Fluorescence based EMSA of DnaA binding to DNA substrates.

(A) The HR13 DNA (1 pmole) was incubated with increasing concentration of DnaA for 5 minutes in the presence of 1mM ADP•BeF_3. From lane 1 to 14, the DnaA concentrations are: 0, 100 nM, 150 nM, 200 nM, 300 nM, 500 nM, 750 nM, 1 µM, 2 µM, 3 µM, 4 µM, 5 µM, 7 µM, 9.17 µM.

(B) The plot of the fraction DNA bound at varying DnaA concentration is given. The equilibrium dissociation constant ($K_{d,app}$) of 2 µM is determined from the Hill equation fitting.

(C) The plot of the fraction DNA bound for OP13 at varying DnaA concentration is given as for HR13. The equilibrium dissociation constant ($K_{d,\,app}$) is 1.6 µM.

(D) The plot of the fraction DNA bound for dT21-ssDNA at varying DnaA concentration (0, 100nM, 200 nM, 300 nM, 500 nM, 750 nM, 1 μM, 2 μM, 3 μM, 4 μM, 5 μM, 7 μM, 8.76 μM). The dissociation constant ($K_{d, app}$) is 2 μM.

(E) The plot of the fraction DNA bound for 18bp-stem at varying DnaA concentration (0, 100nM, 250 nM, 500 nM, 1 μM, 2 μM, 3 μM, 4 μM, 5 μM, 7 μM, 9.06 μM, 18.12 μM, 27.18 μM). The dissociation constant ($K_{d, app}$) is 6.5 μM.

Supplementary Table S1. Ensemble FRET changes before and after adding DnaA in different nucleotides conditions

Nucleotide	***FRET change (pdT21)***
ADP	+6%
ATP	-25%
ATPγS	-25%
ADP•BeF_3	-40%
Without nucleotide	+6%

Supplementary Table S2. Transition rates for the highly populated FRET states of HR and HR-boxes substrates in the presence of 5 μM DnaA and 1 mM ADP•BeF_3.

HR7	State 0↔1	State 1↔2	State 2↔3	State 3↔4
$k_{on(obs)}$ (s^{-1})	0.55	0.4	--	--
k_{off} (s^{-1})	0.53	0.56	--	--

HR10	State 0↔1	State 1↔2	State 2↔3	State 3↔4
$k_{on(obs)}$ (s^{-1})	0.4	0.47	0.4	--
k_{off} (s^{-1})	0.42	0.56	0.5	--

HR13	State 0↔1	State 1↔2	State 2↔3	State 3↔4
$k_{on(obs)}$ (s^{-1})	0.57	0.49	0.43	--
k_{off} (s^{-1})	0.53	0.42	0.59	--

HR13-2box	State 0↔1	State 1↔2	State 2↔3	State 3↔4
$k_{on(obs)}$ (s^{-1})	0.70	0.53	0.44	0.43
k_{off} (s^{-1})	0.42	0.53	0.55	0.65

HR13-5box	State 0↔1	State 1↔2	State 2↔3	State 3↔4
$k_{on(obs)}$ (s^{-1})	--	0.64	0.53	0.55
k_{off} (s^{-1})	--	0.57	0.68	0.77

Supplementary Table S3. DNA substrates

Name	Sequence
Cy5-stem strand	5'-Cy5-GCC TCG CTG CCG TCG CCA-biotin-3'
PIFE-stem strand	5'-GCC TCG CTG CCG TCG CCA-biotin-3'
pdT21-Cy3	5’-TGG CGA CGG CAG CGA GGC TTT TTT TTT TTT TTT TTT TTT-Cy3-3’
pdTcontrol-Cy3	5’-TGG CGA CGG CAG CGA GGC XTT TTT TTT TTT TTT TTT TTT-3’
pdT3+17-Cy3	5’-TGG CGA CGG CAG CGA GGC TTT XTT TTT TTT TTT TTT TTT-3’
HR13-Cy3	5’-TGG CGA CGG CAG CGA GGC TTT TTT TTT TTT TXT TTT TTT TTT TTT TTT TTT TTT TTT TTT TTT TTT TTT TTT TTT-3’
HR10-Cy3	5’-TGG CGA CGG CAG CGA GGC TTT TTT TTT TXT TTT TTT TTT TTT TTT TTT TTT TTT TTT TTT TTT TTT TTT TTT TTT-3’
HR7-Cy3	5’-TGG CGA CGG CAG CGA GGC TTT TTT TXT TTT TTT TTT TTT TTT TTT TTT TTT TTT TTT TTT TTT TTT TTT TTT TTT-3’
HR-2box-Cy3	5’-TGG CGA CGG CAG CGA GGC TTT TTT TTT TTT TXT TTT TTT TAC AGT TTG GGT ATT CGG CTA TTT TCA TTG TTT **TTT TCC ACA** T**TT ATC CAC A**TT TTT A-3’
HR-2box-boxcomplement	5’-TAA AAA TGT GGA TAA ATG TGG AAA A-3’
HR-5box-Cy3	5’-TGG CGA CGG CAG CGA GGC TTT TTT TTT TTT TXT TTT TTT TAC AGT TTG GGT ATT CGG CTA TTT TCA TTG TTT GTC AGC TCT TCA **CTT TCC ACA** AC**T TTT CCA CA**T GAA CAA CTT AAG TTA TTT ATA ATT CGT AAG TTT **TAA GTC ACC** GGA TTG TTT CGT AGT ATG AAT AAC TTA AGA AG**T TTT CCA CA**T **TTA TCC ACA** TTT TTA-3’
HR-5box-boxcomplement	5'-TAA AAA TGT GGA TAA ATG TGG AAA ACT TCT TAA GTT ATT CAT ACT ACG AAA CAA TCC GGT GAC TTA AAA CTT ACG AAT TAT AAA TAA CTT AAG TTG TTC ATG TGG AAA AGT TGT GGA AAG TGA AGA GCT GAC-3'
OP-Cy5-stem strand	5'-biotin-ACC GCT GCC GTC GCT CCG-Cy5-3'
OP-PIFE-stem strand	5'-biotin-ACC GCT GCC GTC GCT CCG-3'
OP13-Cy3	5’-TTT TTT TTT TTT TTT TTT TTT TTT TTT TTT TTT TTT TTT TTT TXT TTT TTT TTT TTT CGG AGC GAC GGC AGC GGT-3’
5’-OP21-Cy3	5’-Cy3-TTT TTT TTT TTT TTT TTT TTT CGG AGC GAC GGC AGC GGT-3’
3’-OP21-Cy3	5’-TTT TTT TTT TTT TTT TTT TTX CGG AGC GAC GGC AGC GGT-3’
dT21-ssDNA (EMSA)	5’-ATTO532-TTT TTT TTT TTT TTT TTT TTT-ATTO647N-3’
18 stem-complement (EMSA)	5’-TGG CGA CGG CAG CGA GGC-3’

X: the position of Cy3 labeling on a C6-Amino-dT base; **Bold with underline part**: Predicted DnaA-boxes from *Aquifex aeolicus oriC* (7)